The Canadian Mineralogist
Vol. 35, pp. 979-998 (1997)

RARE-EARTH-ELEMENT-ACTIVATED CATHODOLUMINESCENCE IN APATITE

ROGER H. MITCHELL[1] AND JIAN XIONG

Department of Geology, Lakehead University, Thunder Bay, Ontario P7E 5B1

ANTHONY N. MARIANO

48 Page Brook Road, Carlisle, Massachusetts 01741, U.S.A.

MICHAEL E. FLEET

Department of Earth Sciences, University of Western Ontario, London, Ontario N6A 5B7

ABSTRACT

Cathodoluminescence (CL) spectra from 350 to 800 nm are presented for synthetic fluorapatite doped with individual rare-earth-element (Ce, Pr, Sm, Eu, Dy, Er) activators. Luminescence peaks in these spectra, together with previously reported data for Tb, Ho and Tm, are assigned to their particular energy-level transitions in the crystal field of apatite. CL spectra obtained on *REE*-doped silicate glasses are used to determine that the approximate sequence of decreasing relative efficiency in luminescence of *REE* activators in the visible light region is Tb, Eu^{3+}, Dy, Sm, Pr, Ce, Ho, Tm, and Er. The interpretation of the CL spectrum of natural apatite on the basis of the CL spectra of apatite doped with single *REE* is deemed simplistic, as an individual *REE* that may give a strong CL where present as the sole activator may not exhibit significant CL in the presence of *REE* of greater efficiency in promoting luminescence. The CL spectra of naturally occurring apatite results from a subtle interplay of at least three major factors: the relative concentration of the individual *REE*, its relative efficiency in promoting luminescence, and the presence or absence of elements that may act as activators, suppressors or co-enhancers of CL.

Keywords: cathodoluminescence, spectrum, apatite, rare-earth elements, luminescence efficiency, alkaline rocks.

SOMMAIRE

Nous présentons des spectres of cathodoluminescence (CL) sur un intervalle de 350 à 800 nm pour la fluorapatite synthétique dopée avec une terre rare (Ce, Pr, Sm, Eu, Dy et Er) agissant individuellement comme activateur. Nous attribuons aux pics de luminescence de ces spectres, considérés à la lumière des données pour Tb, Ho et Tm déjà dans la littérature, les transitions en niveaux d'énergie appropriées pour le champ cristallin de l'apatite. Les spectres CL de verres silicatés aussi dopés avec des terres rares servent à déterminer la séquence approximative de l'efficacité de la série de terres rares à promouvoir la luminescence dans la région visible du spectre; la séquence, décroissante, serait Tb, Eu^{3+}, Dy, Sm, Pr, Ce, Ho, Tm, et Er. Nous croyons que l'interprétation d'un spectre CL d'un échantillon d'apatite naturelle à la lumière d'une série de spectres d'apatite de synthèse dopée avec une seule terre rare est plutôt simpliste. En isolation, une terre rare pourrait donner un effet marqué, qui se trouverait complètement masqué en présence d'autres terres rares ayant une plus grande efficacité de luminescence. Les spectres CL d'échantillons d'apatite naturelle résultent d'une interdépendance subtile d'au moins trois facteurs principaux: la concentration relative d'une terre rare individuelle, l'efficacité relative de la terre rare en question, et la présence ou absence d'autres éléments aptes à activer, supprimer, ou renforcer l'effet de CL.

(Traduit par la Rédaction)

Mots-clés: cathodoluminescence, spectre, apatite, terres rares, efficacité de luminescence, roches alcalines.

INTRODUCTION

Apatite is a common host for minor to trace amounts of rare-earth elements (*REE*) in igneous rocks. The *REE* replace calcium, and their presence typically results in strong extrinsic cathodoluminescence (CL) when the mineral is irradiated by an electron beam (Portnov & Gorobets 1969, Ovcharenko & Yu'ev 1971, Lagerway 1977, Leckebusch 1979, Huaxin 1980, Mariano 1978, 1988, 1989, Dudkin *et al.* 1994). Apatite from various parageneses exhibits distinctive CL colors. For example, apatite hosted by granite typically displays yellow CL, whereas that in carbonatite shows blue CL (Mariano 1988). On the basis of the CL spectra of *REE*- bearing minerals and *REE*-doped

[1] *E-mail address*: rmitchel@gale.lakeheadu.ca

synthetic compounds, including apatite, the different CL colors have been correlated with the presence of particular *REE* activators (Morozov *et al.* 1970, Marfunin 1979, Mariano 1978, 1988, 1989, Roeder *et al.* 1987). However, the assignment of individual luminescence peaks and their relative contributions to the CL spectra of natural apatite to a particular activator remain incompletely understood. Assignment of CL peaks to particular activators by Mariano (1978, 1988) was based on the CL spectra of synthetic apatite doped with *REE* as given by Morozov *et al.* (1970), Nazarova (1961), Steinbruegge *et al.* (1972), and Palilla & O'Reilly (1968). One major problem in such assignments is that individual CL activators have very different efficiencies in producing luminescence. Thus an activator may give prominent peaks in apatite doped with a single *REE*, but these peaks may not be evident when activation occurs in the presence of other *REE* of greater efficiency in producing luminescence. In some instances, significant charge-transfer, crystal-field effects and polarization of the CL spectrum may play a role in determining the character of the observed CL spectrum.

With regard to crystal-field effects, the two Ca positions in the apatite structure at which the *REE* are accommodated have distinct stereochemistries. Fleet & Pan (1994) have noted that the structural role of the *REE* in apatite remains unclear, as a given *REE* may be distributed over both sites. Further, Hughes *et al.* (1991) suggested that La to Pr should prefer the Ca(2) site, whereas Pm to Sm should occupy the Ca(1) site. Clearly, the CL spectrum of any activator sensitive to crystal fields, such as Pr or Ce, will reflect the preferential site-occupancy of the activator. These aspects of the CL of apatite are the least studied and understood.

This work presents new data on the CL of synthetic apatite doped with single *REE* (Xiong 1995) and of synthetic glasses doped with diverse combinations of the *REE*. These data, together with insight from previous studies, especially those of Morozov *et al.* (1970) and Blanc *et al.* (1995), are used to review the interpretation of the CL of naturally occurring apatite and to suggest directions for future studies.

Experimental

Single crystals of fluorapatite containing individual *REE* (Ce, La, Pr, Nd, Sm, Eu, Gd, Dy, Er, Yb, and Lu) at the 0.1 wt.% $(REE)_2O_3$ level were grown from a volatile-rich melt using standard hydrothermal methods, as described by Fleet & Pan (1995, 1994). The maximum size of crystals was about $0.2 \times 0.2 \times 0.2$ mm^3. All crystals were found to be homogeneous by electron-microprobe analysis, back-scattered electron imagery and CL petrography.

CL observations in the visible-light region (350 to 850 nm) were undertaken using a Nuclide Luminoscope (ELM–2B), and CL spectra obtained with a Spex 1681B Minimate spectrophotometer. This instrument is a 0.22-meter, double-dispersion grating spectrometer controlled by a NM–300 computer. All spectra were obtained with a beam voltage of 8–10 keV and a beam current of 0.7–0.8 mA. Low-resolution spectra were obtained with 5-mm entrance and exit slits, whereas maximum sensitivity and resolution were obtained with 0.25-mm slits. Spectra of some synthetic glass standards were obtained with 0.5-mm slits. Changing from a 5 to a 0.25 mm slit width generates a peak shift from 594 to 599 mm for the major Sm^{3+} peak. Spectra were obtained using a fiber-optic probe 1250 μm in diameter and an objective magnification of 10×, giving a sampling area of 125 μm.

The synthetic *REE*-doped apatite samples containing Ce, Pr, Sm, Eu, Dy, and Er emit characteristic luminescence lines or peaks in the visible spectrum under electron-beam irradiation. La, Nd, Gd, Yb and Lu do not exhibit visible-light CL under the conditions of excitation used in this study, although Ozawa (1990) and Morozov *et al.* (1970) have documented ultraviolet or infrared luminescence. Using an excitation potential of 25 kV, Blanc *et al.* (1995) have also concluded that La, Nd, Gd, Yb and Lu do not contribute significantly to the visible-light CL spectrum of apatite. They also observed that Nd gives a strong line in the near-infrared at 875 nm, and Gd produced a very strong line in the near-ultraviolet at 313 nm. Unfortunately, Tb- or Tm-doped apatite that exhibits visible CL (Mariano 1988) was not available for the study by Xiong (1995); however, spectra of such apatite are given by Blanc *et al.* (1995), and are discussed below. Blanc *et al.* (1995) also demonstrated that U may give rise to very strong lines at 300 and 336 nm, in the near-ultraviolet, and confirmed the well-known Mn line at 565 nm.

Cathodoluminescence of *REE*-Doped Apatite

Cerium

Ce-doped apatite exhibits light-blue luminescence, and the CL spectrum consists of a continuous luminescence band centered at 440 nm, with two small superimposed peaks at 593 and 637 nm (Fig. 1A). The difference in energy level between the small peaks is about 0.14 eV.

The absorption and photoluminescence spectrum of synthetic Ce^{3+}-doped apatite reported by Morozov *et al.* (1970) consists of two broad ultraviolet absorption bands at 240 and 310 nm and a photoluminescence broad band at 420 nm. In contrast, Blanc *et al.* (1995) observed a very strong but poorly resolved doublet at 350 and 380 nm, with a broad band at about 458 nm (Fig. 1B). The very weak longer-wavelength peaks observed in this study were apparently absent.

Although the fluorescence of Ce^{3+}-activated compounds has been investigated for many years (Freed 1931, Lang 1936, Henderson & Ranby 1957, Weber & Bierig 1964, Blasse & Bril 1967, Laud *et al.* 1971), no complete crystal-field analysis is available. Thus, the observed CL peaks cannot be unambiguously assigned to particular electronic transitions. The fluorescence emission of Ce^{3+} originates from a transition from one or more of the excited 5*d* levels

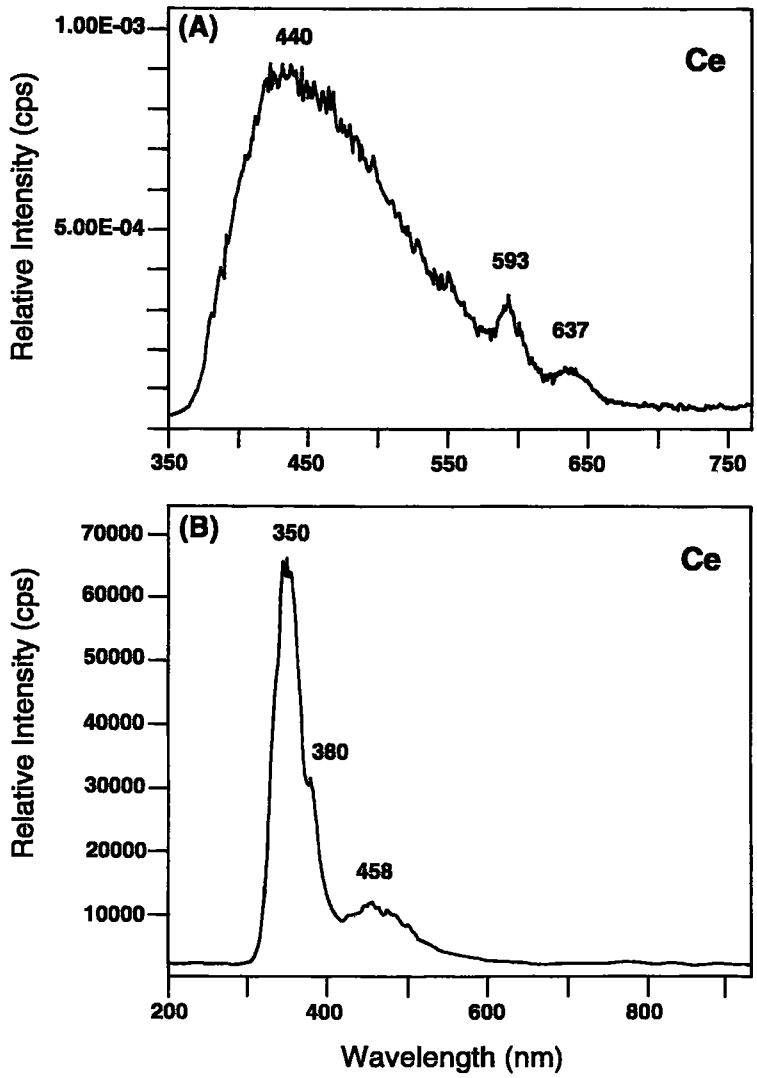

FIG. 1. (A) CL spectrum of Ce-doped apatite (0.18 wt.% Ce_2O_3). Excitation conditions: 8 kV, 0.8 mA, 5-mm slits. (B) CL spectrum of Ce-doped apatite (1 wt.% $CeCl_3 \cdot 6H_2O$) from Blanc *et al.* (1995). Excitation conditions; 25 kV, 10^{-7} A, 0.5-mm slits.

to the ^2F ground state doublet. Blasse & Bril (1967) found that the positions of Ce^{3+}-induced emission peaks in activated phosphors is dependent upon the host's structure. Usually, they lie in the near-ultraviolet for simple oxides, but may occur in the visible region, where the *5d* level is of exceptionally low energy. For example, Ce-doped SrS phosphors exhibit visible peaks, separated by 0.18 eV, at 494 and 532 nm (Keller 1958). These may correspond to transitions from the excited states $^2D_{3/2}$ and $^2D_{5/2}$ (2.51 eV and 2.33 eV) to the doublet ground states $^2F_{5/2}$ and $^2F_{7/2}$, for the $4f^1$ configuration of the Ce^{3+} ion. The 593 and 637 peaks in Ce-doped apatite, which differ by similar energies, also are tentatively assigned to this transition in the crystal field of apatite. The increased wavelength of the peaks, relative to those found for sulfide phosphors, suggests significantly decreased separation of the *f–d* energy levels in phosphate, *i.e.*, reduced spitting, relative to other crystal fields. In addition, the low-symmetry sites occupied by Ce in the apatite structure (Fleet & Pan 1994) may result in splitting of the ^2D energy level into three levels (Keller 1958), with the broad band at 440 nm resulting from the smearing out of the upper two energy levels of the crystal field into a continuum of average energy about 2.81 eV. This conclusion supports those of Blasse & Bril (1967), that the CL spectrum of Ce^{3+} is

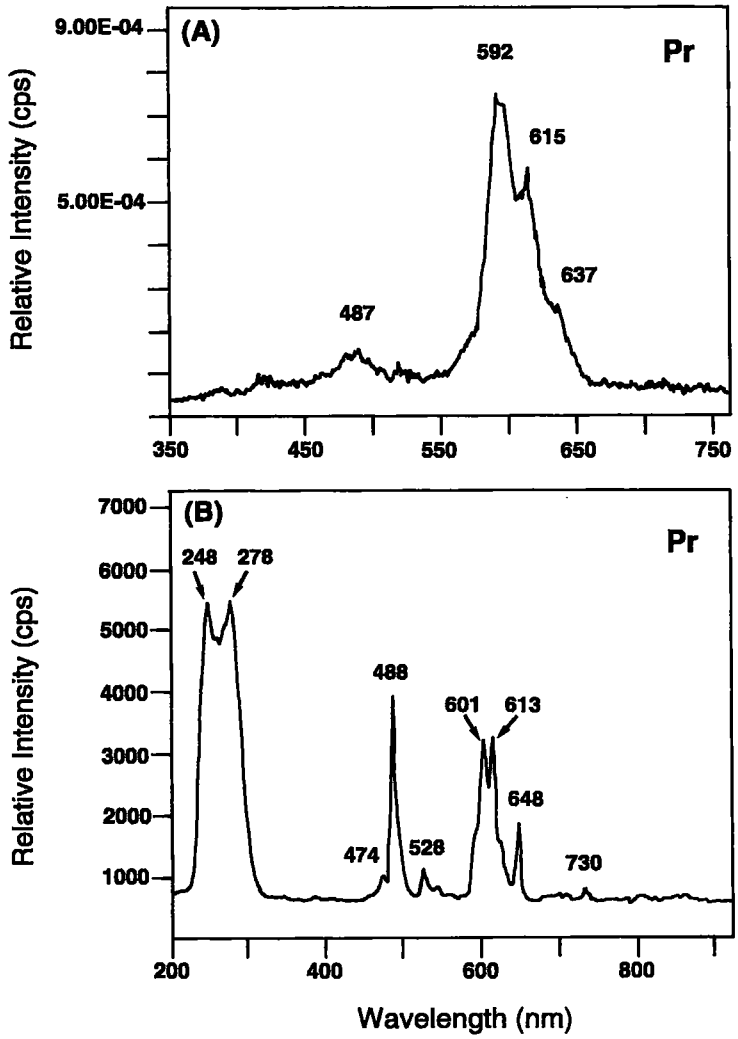

FIG. 2. (A) CL spectrum of Pr-doped apatite (0.19 wt.% Pr_2O_3). Excitation conditions; 8 kV, 0.8 mA, 5-mm slits. (B) CL spectrum of Pr-doped apatite (0.3 wt.% Pr_2O_3) from Blanc *et al.* (1995). Excitation conditions: 25 kV, 10^{-7} A, 0.5-mm slits.

strongly affected by the local crystal-field. Differences in the spectra obtained by Xiong (1995), Blanc *et al.* (1995) and Morozov *et al.* (1970) may arise from different site-occupancies of Ce in the apatite structure or from defects in the structure, giving rise to intrinsic luminescence.

Praseodymium

Pr-doped apatite shows brick-red luminescence, and the CL spectrum consists of a weak peak at 487 nm plus an intense unresolved band consisting of three peaks located at 592, 615 and 637 nm (Fig. 2A). There is an indication of a peak at about 522 nm, but this could not be resolved from the background, even using 0.25 mm slits. The peak at about 428 nm is not a Pr line, but probably represents a line in the background spectrum of the cold cathode electron gun.

Morozov *et al.* (1970) reported that the photoluminescence spectrum of Pr- doped apatite consists of three groups of lines in the blue (450–500 nm), red (600–710 nm) and infrared (850–910 nm) regions. In the visible spectrum, our data are in broad agreement with these assignments, with the recognition of a weak band at 450–500 nm, and a more intense band at 600–650 nm, hence the overall red CL color. However, we did not observe the lines about 680 and 715 nm reported by Morozov *et* al. (1970).

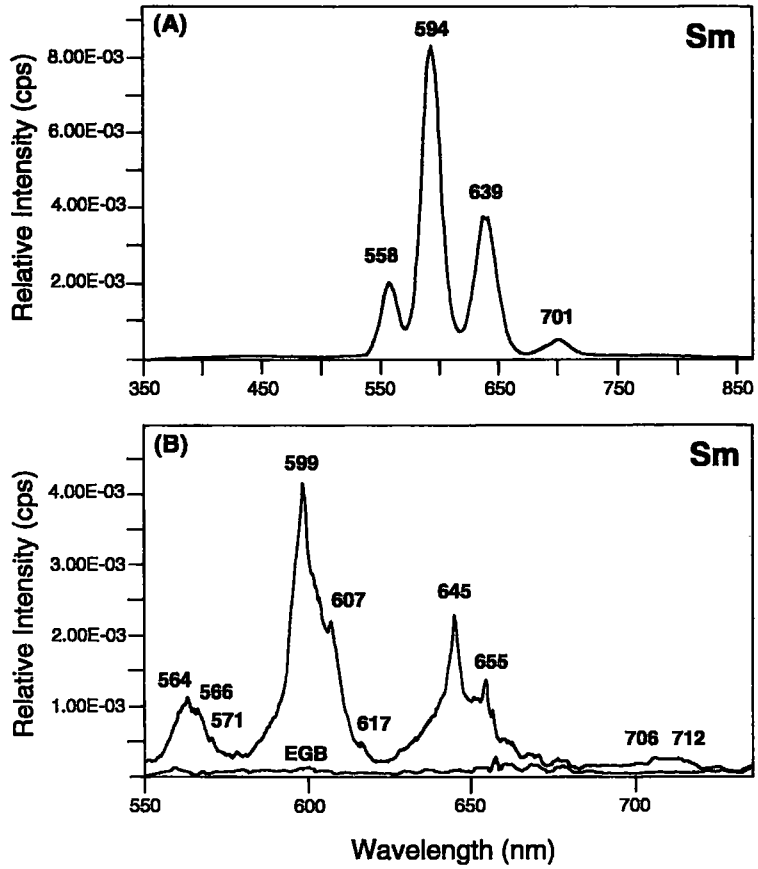

FIG. 3. (A) CL spectrum of Sm-doped apatite (0.16 wt.% Sm_2O_3). Excitation conditions; 8 kV, 0.8 mA, 5-mm slits. (B) High-resolution CL spectrum of Sm-doped apatite between 550 and 730 nm, plus the background spectrum of output from the cold cathode electron gun (EGB). Excitation conditions: 8 kV, 0.8 mA, 0.25-mm slits.

Visible-light spectra obtained by Blanc *et al.* (1995) are similar in that they observe a poorly resolved doublet at 601 and 613 nm. Their data differ in that they observed a large peak at 488 nm instead of the weak band found in our study, together with a significant well-resolved peak at 648 nm (Fig. 2B). Blanc *et al.* (1995) also reported a very strong ultraviolet doublet at 248 and 278 nm. These differences no doubt arise from the higher excitation potential (25 kV) employed by Blanc *et al.* (1995) (8 kV in our study).

The Pr^{3+} spectra are in agreement with those previously found for a variety of Pr-doped compounds (Sayre *et al.* 1955, Sayre & Freed 1955, Dieke & Crosswhite 1963, Gravely 1970, Dornauf & Heber 1979, Mariano 1988). However, Pr spectra show significant crystal-field (Fig. 2) and columinescence (Dornauf & Heber 1979) effects, which together may result in significant differences in Pr spectra and relative intensities of peaks in different hosts.

Intense luminescence peaks of Pr^{3+} in the red region may be assigned to transitions between the two lowest energy-levels ^3F and ^3H, and the upper levels $^3P_{0,1}$ and $^1D_2$ in the $4f^2$ configuration (Dieke & Crosswhite 1963, Dornauf & Heber 1979). The transitions from the lowest ground-level $^3H_4$ to the upper P and D levels are represented by the weak band and strong peak at 487 nm and 592 nm, respectively. The higher-wavelength peaks at 615 and 637 nm represent transitions among the $^3H_6$ and $^3F_2$ and $^3P_{0,1}$ levels, respectively.

It is important to note that although the major luminescence-induced peaks for Pr^{3+} are coincident with those of Sm^{3+}, the two elements may have very different efficiencies in producing luminescence (see below).

Samarium

Sm-doped apatite exhibits an orange-red luminescence. The low-resolution spectrum collected with 5-mm slits consists of four groups of bands located approximately at 558, 594, 639 and 701 nm (Fig. 3A). Using 0.25-mm slits, these bands may be partially resolved into groups of discrete peaks accompanied by a wavelength shift of 5–6 nm (Fig. 3B).

The luminescence band at 558 nm (5-mm slits) consists of three low-intensity peaks at 564, 566 and 571 nm. The most intense band at 594 nm (5-mm slits) consists of three lines, at 599, 607 and 617 nm. The band at 639 nm (5-mm slits) consists of two lines at 645 and 635 nm, and the weak band near the infrared at 701 nm (5-mm slits) consists of two very weak peaks, at 706 and 712 nm.

Our spectrum of Sm-activated apatite is similar to spectra obtained by Marfunin (1979) and Morozov *et al.* (1970); these consist of numerous narrow lines distributed in groups at 545–560, 585–605, 635–655 and 720–750 nm. The relatively low-resolution spectrum of Sm-doped apatite reported by Blanc *et al.* (1995) does not differ significantly from that obtained in our study, although they reported a weak peak superimposed on a broad band at 803 nm. Their study, the present work and the spectra of Sm-activated phosphors (Ozawa 1990) demonstrate that the most intense peak of Sm^{3+} is always the highest-energy peak (ranging from 594 to 608 nm) of the 590–620 nm region. In contrast, Morozov *et al.* (1970) indicated that the most intense peak of Sm^{3+}-activated apatite lies at about 650 nm. The discrepancy is due to the differing modes of excitation employed in the different investigations.

The luminescence of Sm^{3+}-activated apatite results from a plethora of *f–f* electronic transitions. Axe & Dieke (1962) and Wybourne (1962) noted that the 73 multiplets of the Sm^{3+} $4f^5$ configuration give rise to 198 energy levels through spin–orbit interactions. As the positions and intensities of the luminescence lines in apatite are very similar to those found in Sm-doped LaF_3 and $LaCl_3$ (Rast *et al.* 1967, Magno & Dieke 1962), and samarium phosphate glass (Farok *et al.* 1992), it is possible to identify approximately the electronic transitions giving rise to the apatite CL spectrum. Sm-doped LaF_3 in particular provides a useful guide to transition assignment, as the site symmetry of Sm is similar to that of Sm replacing Ca in apatite. In general, luminescence due to Sm^{3+} is associated with transitions from the ^4G and ^4F excited states to the ground state ^6H multiplet. Unfortunately, postulated energy-levels are numerous and closely spaced (Magno & Dieke 1962, Rast *et al.* 1967). Thus transition assignments are not simple, and are not unambiguous when pronounced crystal-field effects may be present.

Bearing the above comments in mind, the high-energy group of lines at 564, 566 and 571 nm (0.25 mm slits) may be assigned to transitions from $^4G_{5/2}$ to $^6H_{5/2}$, $^4F_{3/2}$, and $^4G_{7/2}$ to $^6H_{9/2}$, respectively. The intense peak at 599 nm (0.25 mm slits) is probably due to the $^4G_{5/2}$ to $^6H_{7/2}$ transition, with the associated peaks at 607 and 617 nm (0.25-mm slits) being due to transitions from $^4F_{3/2}$ to $^6H_{9/2}$ and $^4G_{7/2}$ to $^6H_{11/2}$, respectively. The 645 and 655 nm lines (0.25-mm slits) may result from $^4G_{5/2}$ to $^6H_{9/2}$ transitions, and the weak low-energy peaks at 706 and 712 nm (0.25-mm slits), from transitions from $^4G_{5/2}$ to $^6H_{11/2}$ (Farok *et al.* 1992).

Europium

Eu-doped apatite typically shows very bright light-blue luminescence. Some crystals observed in this study initially showed a light violet-blue luminescence which, after prolonged electron-beam irradiation, changed to the more common light-blue color. The CL spectrum obtained using 5-mm slits consists of three relatively weak, low-energy narrow peaks (587, 612, 694 nm) and a high-energy broad peak centered at 450 nm (Fig. 4A). The intensity of this broad peak is inversely proportional to the duration of electron-beam irradiation. Higher-resolution spectra (Fig. 4B) obtained using 0.25-mm slits resolve the most intense single band at 612 nm (5-mm slits) into three lines, located at 615, 619 and 622 nm. The band at 587 (5-mm slits) can be resolved into three lines at 589, 592 and 596 nm. The band at 694 nm (5-mm slits) consists of two weak peaks, at 697 and 702 nm.

Eu-doped apatite studied by Morozov *et al.* (1970) shows strongly polarized red photoluminescence associated with peaks in the 600–650 nm region. The significant difference in luminescence color with respect to that observed in this work stems from inability of the mercury lamp used by Morozov *et al.* (1970) to stimulate the strong high-energy transition at 450 nm observed with electron irradiation. The spectrum of Eu-doped apatite reported by Blanc *et al.* (1995) is similar to that we obtained, in that four peaks may be recognized; however, this spectrum differs in that the peak at 451 nm is the only strong one.

Interpretation of spectra obtained from Eu-activated apatite is complicated by the fact that Eu may occur as the Eu^{2+} or Eu^{3+} ion. Although the luminescence spectra of both ions are produced by the same type of *f–f* transitions, they are quite different, as the Eu^{2+} ion produces a broad emission band in the blue region, and the Eu^{3+} ion gives a series of narrow peaks in the red region (Marfunin 1979). Apatite containing Eu in both valency states consequently exhibits complex spectra (Mariano & Ring 1975, Roeder *et al.* 1987, Mariano 1988, 1989). Synthetic apatite that contains exclusively Eu^{2+} or Eu^{3+} has apparently not been synthesized, and even that crystallized under low fugacity of oxygen show CL peaks due to Eu^{3+} (Mariano 1988, Roeder *et al.* 1987). The apatite studied by Blanc *et al.* (1995) was synthesized under reducing conditions and, from the character of its spectrum, must contain predominantly Eu^{2+}.

Roeder *et al.* (1987) and Mariano (1988) attributed CL peaks at 585–590, 613–615, 645, 690–700 nm to Eu^{3+} activation, and the band at 450 nm, to Eu^{2+} activation. These assignments were verified with CL spectra of

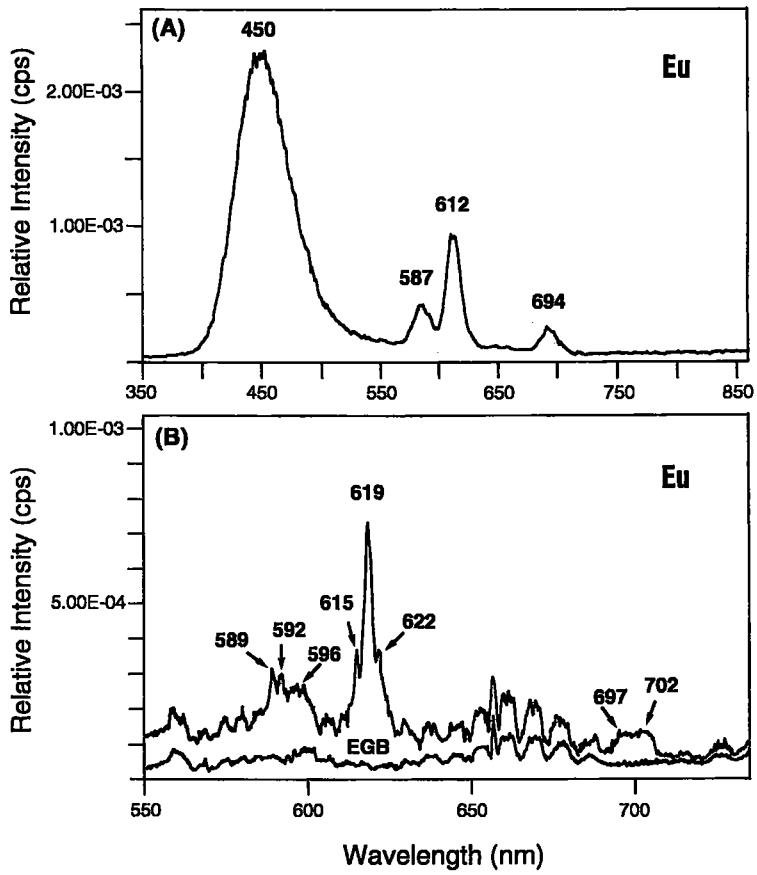

FIG. 4. (A) CL spectrum of Eu-doped apatite (0.14 wt.% Eu_2O_3). Excitation conditions: 8 kV, 0.8 mA, 5-mm slits. (B) High-resolution spectrum of Eu-doped apatite from 550 to 730 nm, plus the background spectrum of output from the cold cathode electron gun output (EGB). Excitation conditions: 8 kV, 0.8 mA, 0.25-mm slits.

Eu-doped glasses formed under varying fugacities of oxygen (Roeder *et al.* 1987). These data demonstrated that decreasing fugacity of oxygen is accompanied by increasing intensity of the blue band at 450 nm with concomitant decrease in intensity of the peaks in the red region.

The Eu-doped compositions of apatite synthesized in this work contain only Eu_2O_3 in the starting materials. However, no attempt was made to control oxygen fugacity during the synthesis. The CL spectrum demonstrates that reduction of much of the Eu to the divalent state occurred during synthesis, as the peaks may be assigned according to the suggestions of Roeder *et al.* (1987). Consequently, the CL spectrum is similar to that of synthetic Eu-doped apatite illustrated by Mariano (1988).

The luminescence lines of Eu^{3+} of apatite are similar to those found in Eu-doped oxides, halides and phosphors (DeShazer & Dieke 1963, Brecher *et al.* 1967, Ropp 1964, Ozawa 1990, Toda *et al.* 1997). The Eu^{3+} ion in the $4f^6$ configuration has 119 multiplets, which yield 295 energy states through spin–orbit interaction. In this configuration, Eu^{3+} has three low-energy excited states ^5D_j (j = 0,1,2) and a ground-state multiplet ^7F_j, consisting of seven spin-orbit states (j = 0–6) (Dieke & Crosswhite 1963). The luminescence lines of Eu^{3+} in apatite may be identified by comparison with the energy levels observed in Eu-doped *REE* halides. The weak line at 580 nm can be assigned to the transition from lowest excited state.The lines from 589 to 596 nm probably reflect $^5D_0$ to $^7F_1$ transitions. The lines from 615 to 619 are generally assigned to the $^5D_0$ to $^7F_2$ transition. The $^7F_2$ level consists of three non-degenerate (A_1, B_1, B_2) and one degenerate (E) sublevels (Brecher *et al.* 1967). The B_2 and E levels

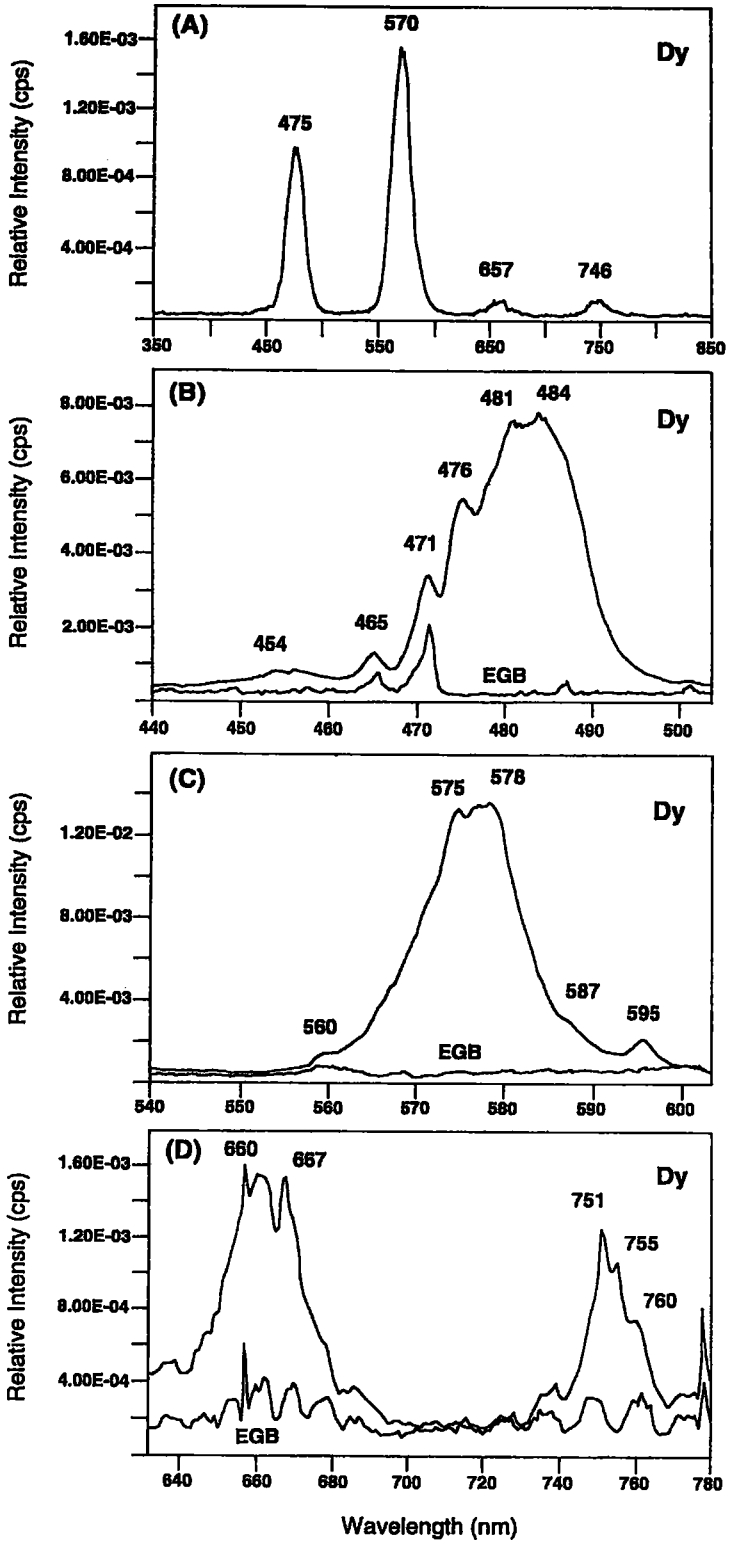

FIG. 5. (A) CL spectrum of Dy-doped apatite (0.12 wt.% Dy_2O_3). Excitation conditions: 8 kV, 0.8 mA, 5-mm slits. (B), (C) and (D) High-resolution CL spectra of Dy-doped apatite in the 440–510 nm, 540–610 nm and 620–780 nm regions, respectively, plus the background spectrum of output from the cold cathode electron gun (EGB). Excitation conditions: 8 kV, 0.8 mA, 0.25-mm slits.

are an electric dipole and have been identified by Brecher *et al.* (1967) as the $^5D_0$ to $^7F_2$ transition of Eu^{3+} in YVO_4. This dipole shows a polarized component along the *c* axis at 615.5 nm and a perpendicular component at 619.4 nm. Transitions to the other two sublevels are optically forbidden. In our studies, most of the Eu-doped apatite grains were oriented parallel to the *c* axis, and the spectra are obtained with the emitted light propagated nearly perpendicular to this axis. Thus the spectra reveal the nondegenerate transitions, which show a higher intensity at the 619 nm line than at the 615 nm line. The line at 622 nm may represent the $^5D_1$ to $^7F_4$ transition, whereas the lower-energy peaks at 697 and 702 may represent $^5D_0$ to $^7F_4$.

The intense band at 450 nm could not be resolved using the 0.25-mm slits. As the intensity of this band exhibits time-related decay, it is attributed to either a perturbed energy-level of the activator (Ropp 1964) or Eu^{2+} to Eu^{3+} charge-transfer interactions (Ozawa 1990).

Dysprosium

Dy-doped apatite exhibits a light creamy yellow luminescence. The CL spectrum at low resolution consists of four bands centered at 475, 570, 657, and 746 nm (Fig. 5A). Higher-resolution spectra show that the band at 475 nm (5-mm slits) is resolved into four Dy-related peaks located at 457, 476, 481 and 484 nm (Fig. 5B) plus two peaks attributed to cathode-ray-tube output at 465 and 471 nm. Figure 5C indicates that the peak at 570 nm (5-mm slits) is resolved into three Dy-related peaks at 575, 578 and 595 nm. The shape of the high-energy shoulder of the 575–578 nm doublet suggests that a further unresolved peak exists at about 570 nm. The weak peak at 560 nm is a line due to electron-gun background. Figure 5D shows that the peak at 657 nm (5-mm slits) is a doublet (660, 667 nm), and the one at 746 nm (5-mm slits) is a triplet (751, 755, 760 nm). These peaks may be enhanced by lines due to electron-gun background in this region of the spectrum.

The spectrum of Dy-doped apatite obtained in this work is similar to the photoluminescence spectrum of Dy-activated apatite obtained by Morozov *et al.* (1970), and is identical to the low-resolution spectrum obtained by Blanc *et al.* (1995) after instrumental peak-shifts are taken into account. The Morozov *et al.* (1970) spectrum consists of five groups of lines in the wavelengths ranges of 470–500, 570–600, 650–700, 750–800 and 850 nm. Similar CL spectra have been observed for Dy-doped YVO_4, La_2O_3 and La_2O_2S (Ozawa 1990). The CL spectra of the latter two compounds contain lines at 570–571 nm.

Mariano (1988) noted that the major Dy lines in apatite occur at 480 and 575 nm, in general agreement with this work. Importantly, the major Dy line at 570 nm is nearly coincident with the 558 nm Sm line. Figures 8.5 of Mariano (1988) demonstrates that these peaks may not be resolved in low-resolution spectra. The efficiency of activation for these two ions has been found by Buchanan *et al.* (1967) to be approximately the same in Y_2O_3.

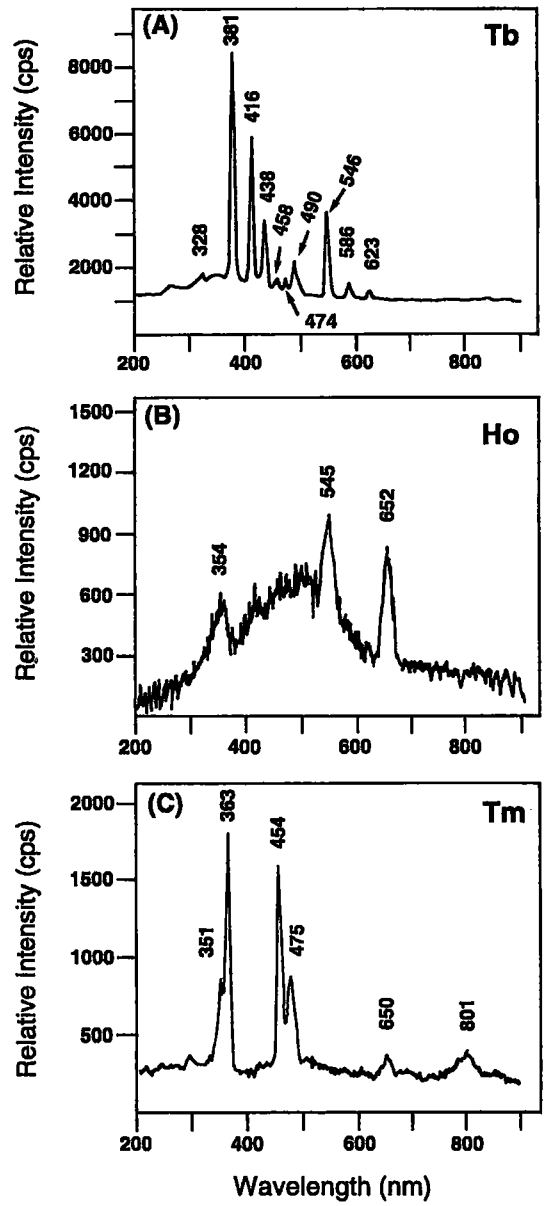

FIG. 6. CL spectra of (A) Tb-doped apatite (0.1 wt.% Tb_2O_3), (B) Ho-doped apatite (1 wt.% Ho_2O_3), (C) Tm-doped apatite (1% Tm_2O_3). All data from Blanc *et al.* (1995). Excitation conditions: 25 kV, 10^{-7} A, 0.5-mm slits.

Interpretation of the luminescence of the Dy^{3+} ion in the $4f^9$ configuration is complicated by the large number of energy levels present in the ground state and lowest excited-states multiplets (Crosswhite & Dieke 1961, Wybourne 1962, Crosswhite & Moos 1967). Tentative assignments suggest that the 476 and 481 nm lines

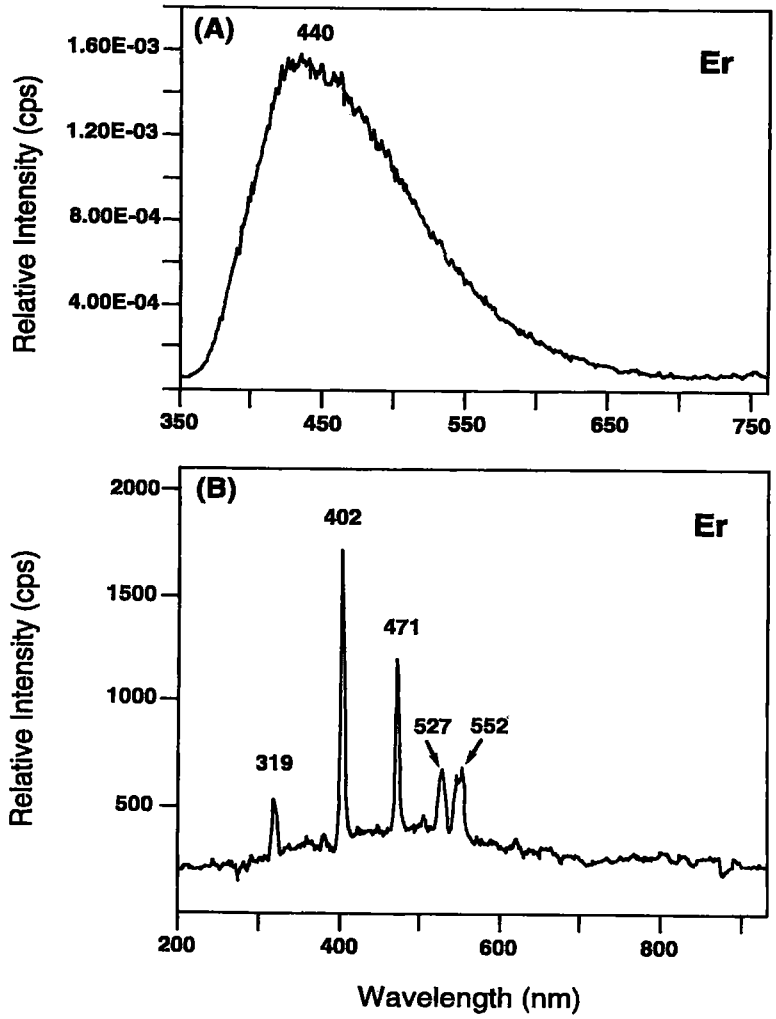

FIG. 7. (A) CL spectrum of Er-doped apatite (0.09 wt.% Er_2O_3). Excitation conditions: 8 kV, 8 mA, 5-mm slits. (B) CL spectrum of Er-doped apatite [1.5% (2NaCl + Er_2O_3)] after Blanc *et al.* (1995). Excitation conditions: 25kV, 10^{-7} A, 0.5-mm slits.

reflect transition from the lowest-energy excited level $^4F_{9/2}$ to the lowest ground-state level $^6H_{15/2}$. Peaks at 575, 660, and 751 nm may be assigned to transitions from $^4F_{9/2}$ or $^6F_{11/2}$ to $^6H_{13/2}$, $^6H_{11/2}$ and $^6H_{9/2}$, respectively. These ground-state levels must be composed of non-degenerate sublevels to account for the presence of the doublets and triplet observed in the high-resolution spectrum. Peaks at 457, 484, 578 and 667 nm are wide and diffuse, and represent emission from the higher Stark components of the electronic levels I, L, T, and O.

Terbium

The CL spectrum of Tb-doped apatite (Fig. 6A) obtained by Blanc *et al.* (1995) is in broad agreement with the photoluminescence (PL) spectra reported by Morozov *et al.* (1970), with a group of lines at 350–425 nm and a strong line at about 545 nm. These correspond to transitions from the excited states $^5D_3$ and $^5D_4$ to the $^7F_6$ and $^7F_5$ ground-state multiplets, respectively (Hayakawa *et al.* 1996). The states $^5D_3$ and $^5D_4$ are separated by an energy gap of about 5600 cm^{-1}, and which is similar to

that observed in Tb-doped $LaCl_3$ and CaF_2 (Dieke & Crosswhite 1963, Marfunin 1979). Morozov *et al.* (1970) noted that the PL spectra of Tb-doped apatite are polarized. Hayakawa *et al.* (1996) have also demonstrated significant concentration-quenching effects upon transitions involving the ^5D_j to $^7F_5$ multiplets at 540–550, 560–580 and 610–625 nm.

Holmium

The spectrum of Ho-doped apatite (Fig. 6B) presented by Blanc *et* al. (1995) consists of three weak peaks at 652, 545 and 354 nm superimposed upon a broad band centered at about 500 nm. The strongest peaks at 652 and 545 can be ascribed to transitions from $^5F_4$ and $^5F_5$ to the ground state $^5I_8$ (Farok *et al.* 1996). As the luminescence efficiency of Ho in apatite is very weak, even the strongest peaks cannot be expected to contribute significantly to the spectra of natural samples containing more efficient activators, such as Sm or Eu.

Erbium

Er-doped apatite exhibits light-blue luminescence. The spectrum consists of a single broad band centered at about 440 nm (Fig. 7A). This spectrum is very similar to that of Ce^{3+}-doped apatite (Fig.1), but lacks any well-defined low-energy peaks.

Spectra of Er-activated apatite obtained by Morozov *et al.* (1970) show no visible or infrared photoluminescence. In contrast, Blanc *et al.* (1995) observed five well-resolved peaks at 319, 402, 471, 527 and 552 nm (Fig. 7B). The absence of discrete Er^{3+} lines in our spectrum and that of Morozov *et al.*(1970) is surprising, given that sharp lines are found in phosphors in the 350–400 and 500–600 nm regions (Ozawa 1990), Er-activated $CaWO_4$ (Van Uitert & Johnson 1966) and Er-doped glasses (Tanabe *et al.* 1995). Their absence in our study is no doubt related to the poor efficiency of luminescence induced by Er; we conclude that the transitions responsible for these lines are not activated at an operating voltage of 8 kV. The peaks at 552 and 527 observed by Blanc *et.* (1995) are attributable to $^4S_{3/2}$ and $^2H_{11/2}$ transitions to the $^4I_{15/2}$ ground state (Tanabe *et al.* 1995).

Thulium

Photoluminescence (Morozov *et al.* 1970) and CL spectra (Fig. 6C) of Tm-doped apatite presented by Blanc *et al.* (1995) consist of strong lines in the blue region (351, 361, 454, 475 nm) and three groups of very weak bands in the orange-red region (centered at 650 and 800 nm). The latter represent transitions from $^1D_2$ to $^3H_4$ and $^3F_2$, and from $^1G_4$ to $^3H_6$, with the strong lines at 454 and 361 nm being due to the $^1D_2$ to $^3F_4$ and $^1D_2$ to $^3H_6$ transitions, respectively (Tanabe *et al.* 1995, Ozawa 1990, Morozov *et al.* 1970). The luminescence efficiency of Tm is weak relative to other rare earths, and the strongest lines in the blue region may be expected only in apatite rich in the heavy *REE*.

Luminescence Efficiency – Cathodoluminescence Spectra of Glasses

The luminescence efficiency of the *REE* activators varies considerably, with the *REE* at the midpoint of the lanthanide series exhibiting the most intense activation in the visible and ultraviolet regions. In contrast, the light and heavy *REE* are the most intense infrared emitters (Buchanan *et al.* 1967). The efficiency of luminescence for the individual *REE* in a particular host can be measured in synthetic materials where only one of the *REE* occurs at a fixed concentration.

However, these data may not be entirely relevant to natural minerals in which the *REE* occur as a coherent group, with wide variation in their relative concentrations. Whereas a single *REE* in a specific host may function as an activator, in the presence of other *REE* it may serve either as a sensitizer, transferring absorbed excitation-energy to another activator, with or without itself emitting luminescence energy (*e.g.*, Gd enhancement of Eu fluorescence: Dornauf & Heber 1979), or it may quench the emission of another *REE*, (*e.g.*, Er quenching of Nd fluorescence: Pelletier-Allard *et al.* 1994). There is also the possibility that *REE* present in high concentrations may exhibit self-quenching; for example, the silicate apatite $Na_2Pr_8Si_6O_{24}F_2$ synthesized by Ito (1968) shows no CL (Mariano, unpubl. data).

A good test for estimating the relative efficiency of luminescence of the *REE* can be made by measuring the CL spectra of synthetic silicate glasses containing equal amounts of *REE*. As we consider that the *relative* efficiency of luminescence is essentially site-independent, we believe that these data are directly relevant to an understanding of *REE*-activated CL in apatite and other luminescent minerals.

Figure 8 shows CL spectra of two *REE*-bearing silicate glass standards synthesized by Roeder (1985). The spectra in Figure 8A, for glass containing 800 ppm each of the *REE* (La–Lu), show CL line emissions only for Tb^{3+}, Eu^{3+}, Sm^{3+} and Dy^{3+}. All other *REE* are not activated. Terbium shows the highest efficiency, followed by Eu, with Sm and Dy having lower and similar efficiencies. The poor resolution in the area between 550 and 590 nm is a result of the coalescence of line emissions from Eu, Dy and Sm. The spectrum of glass containing 1 wt.% each of the *REE* (Fig. 8B) differs significantly in that the Tb emissions in the blue part of the spectrum are absent, and the Eu peak is greatly enhanced. We suggest that the higher concentrations of Tb may give rise to incipient self-quenching, and that Eu emission is enhanced by charge transfer from non-luminescing activators.

Spectra for four *REE*-bearing Ca–Al silicate glasses prepared by D.L. Hamilton (University of Manchester, U.K.) are illustrated in Figure 9. In these glasses, the *REE* occur at the 4 wt.% level, and fortuitously, each of the

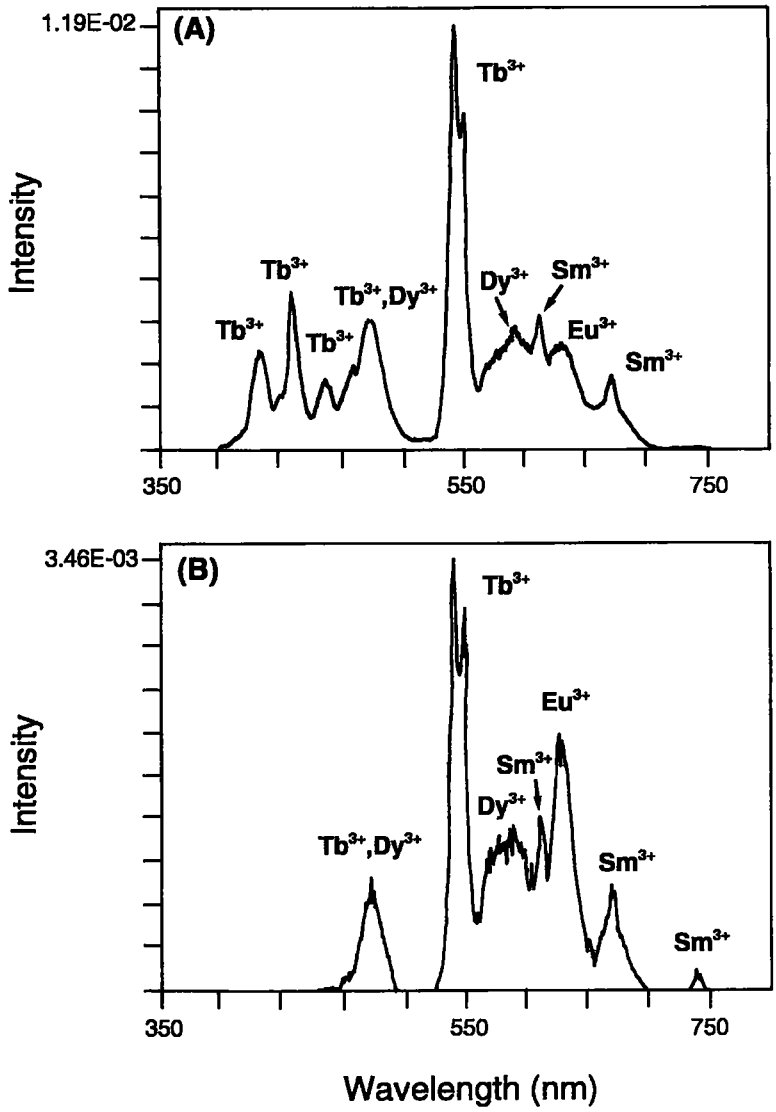

FIG. 8. CL spectra of silicate glass standards containing *REE*, prepared by Roeder (1985). (A) Glass S–253 with La–Lu each at the level of 800 ppm *REE*. (B) Glass S–254 with La–Lu each at the level of 1.0 wt.% *REE*. Excitation conditions: 5 kV, 0.9 mA, 0.5-mm slits.

REE activators that are the most efficient emitters are isolated from each other. The spectra were obtained under the same experimental conditions and, therefore, the relative efficiency of luminescence can be directly observed. Tb is the strongest emitter, followed by Eu^{3+}, whereas Dy and Sm are less efficient. Figure 9C shows that there is only minor luminescence from the major line emissions of Pr and Er, which demonstrates that compared to Sm, Eu, Dy and Tb, these elements are relatively weak CL activators. This is important, given that the major lines of Pr and Sm are of similar wavelength. Note that the Tb lines of shorter wavelength than 570 nm shown in Figure 9D are virtually identical to those in Figures 6A and 8A and to those found in a variety of Tb-doped synthetic tungstates, fluorides and phosphates (Ozawa 1990); thus Tb-induced CL seems to be essentially independent of the crystal fields, but may be dependent upon concentration.

Finally, another four silicate glasses prepared by Drake

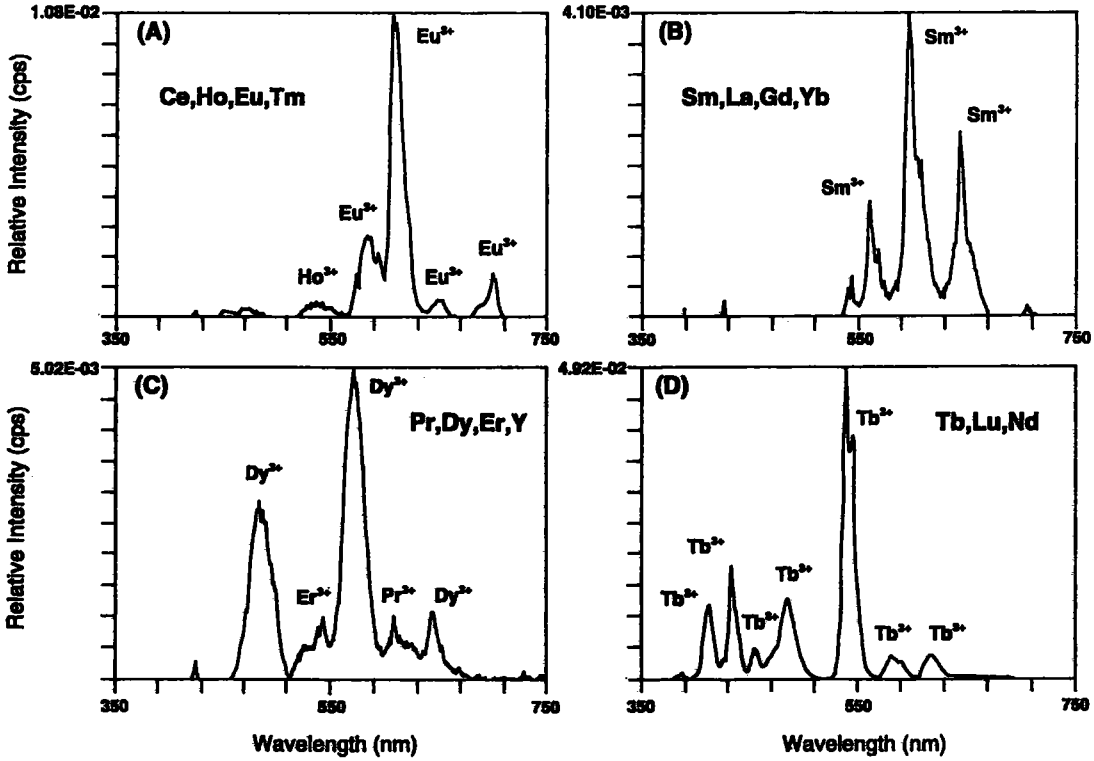

FIG. 9. CL spectra of *REE*-doped Ca–Al silicate glasses prepared by D.L.Hamilton. All glasses contain each *REE* at the 4.0 wt.% level. Luminescence efficiency decreases in the order Tb, Eu^{3+}, Sm, Dy, Pr, Er. Excitation conditions: 5 kV, 0.9 mA, 0.5-mm slits.

& Weill (1972) provide an informative comparison with those prepared by Hamilton; although the *REE* occur at approximately the same level of concentration, they are present in a different combination. The spectra illustrated in Figure 10 show that the luminescence efficiency for the *REE* activators is essentially in the same order as determined from Hamilton's glasses. However, Figure 10C shows that prominent Pr peaks, together with a small Ce^{3+} peak, are evident in glass *REE*3, which does not contain any of the efficient *REE* activators. These observations indicate that where Pr or Ce occur in the presence of such activators (Figs. 8, 9A, 9C), they cannot contribute significantly to the CL spectrum.

APPLICATION TO NATURALLY OCCURRING APATITE

The studies of Xiong (1995) and Blanc *et al.* (1995) demonstrate that the CL spectra of *REE*-activated synthetic apatite in the visible to near-infrared region *may* contain peaks and bands reflecting the presence of Ce, Pr, Sm, Eu^{2+}, Eu^{3+}, Gd, Tb, Dy, Ho, Er and Tm. The wavelengths of the major emission lines and bands are listed in Table 1. Naturally occurring apatite displays a very wide range of CL colors, but not all of the emission lines possible are evident in their CL spectra. Furthermore, many of the "peaks" in the apatite CL spectrum are in reality composite bands.

Mariano (1978, 1988, 1989) has demonstrated that the diverse CL colors of naturally occurring apatite reflect differing proportions of CL activators. In addition to

TABLE 1. CL CHARACTERISTICS OF APATITE OVER THE INTERVAL 350–800 nm

Wavelength	Activator	Wavelength	Activator
350 nm	Ce	565 nm	Mn
380	Ce	575	Dy
381	Tb	587	Eu^{3+}
402	(Er)	592	Pr
438	Tb	593	Ce
440	Ce, (Er)	594	Sm
450	Eu^{2+}	612	Eu^{3+}
471	(Er)	615	Pr
474	Tb	637	Pr*
480	Dy	639	Sm
487	Pr	652	(Ho)
490	Tb*	657	Dy*
545	(Ho)	694	Eu^{3+}
546	Tb	701	Sm
558	Sm	746	Dy*

All *REE* except Eu are considered to be trivalent ions. The activators that have a very poor efficiency in promoting luminescence are shown in parentheses. *: weak lines or bands.

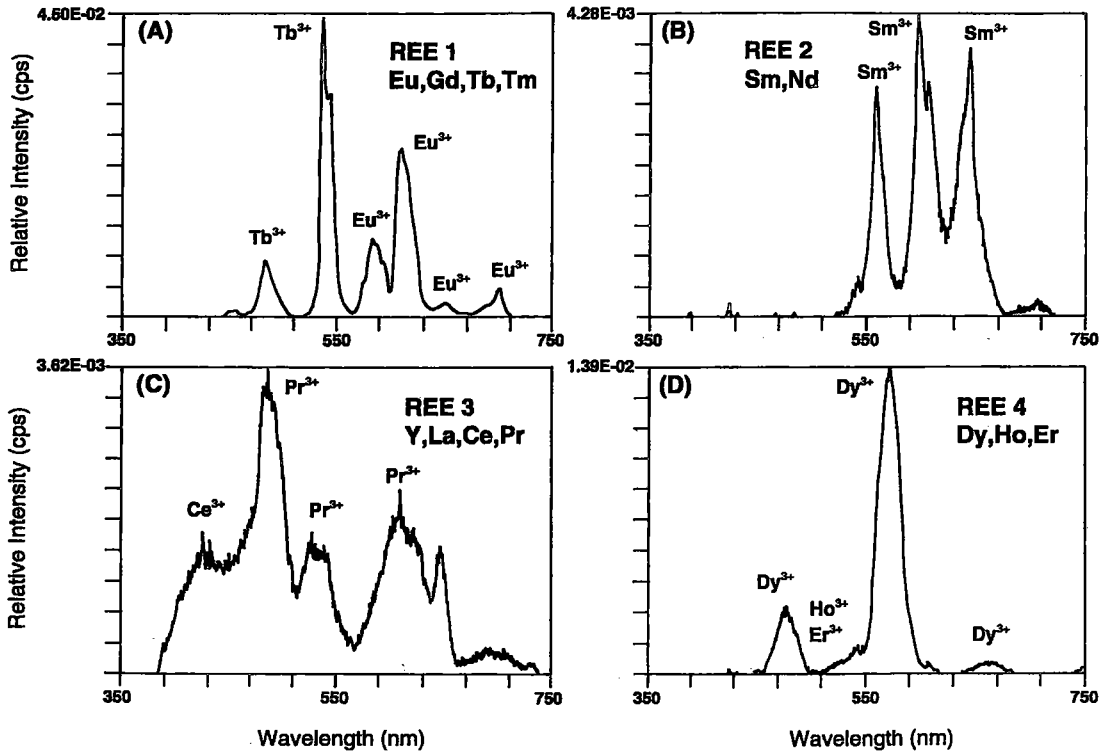

FIG. 10. CL spectra of *REE*-doped Ca–Al silicate glasses prepared by Drake & Weill (1972). Glasses contain each *REE* at the 4.0 – 4.46 wt.% level. Luminescence efficiency decreases in the order Tb, Eu^{3+}, Dy, Sm. Pr, Ce, Ho, Er. Note that although Drake & Weill (1972) reported Eu in glass *REE*1 as EuO, the CL spectrum shows only Eu^{3+} peaks. Excitation conditions: 5 kV, 0.9 mA, 5-mm slits.

the *REE*, he has also shown that Mn is an important activator, and its presence results in a single peak located at 565 nm. This peak is close to the 540, 558, and 570 nm peaks of Tb, Sm and Dy, respectively, and may completely mask these lines if these *REE* are present in small quantities.

The data obtained in the present study and by Blanc *et al.* (1995) indicate that the peak assignments suggested by Mariano (1978, 1988, 1989) for *REE*-activated apatite are essentially correct. However, taking into consideration our data on the relative efficiency of luminescence of *REE* activators, we propose that the CL spectrum of a particular natural sample of apatite results from the subtle interplay of a least three major factors: (1) the relative concentrations of the individual *REE*, (2) the relative efficiency of luminescence of the *REE* present, and (3) the presence or absence of other CL activators (*e.g.*, Mn).

It is particularly important to note that some of the most efficient CL activators that may be present in very low concentrations are the dominant contributors to the CL spectrum. Furthermore, our studies suggest that Ce and Pr may play a role in the generation of the overall CL spectrum only where more efficient activators are not present. Thus Blanc *et al.* (1995) have demonstrated the presence of the strong Ce peaks at 350 and 380 nm in several natural samples of apatite originating from light-*REE*-rich environments.

Pr is enriched in many samples of apatite compared to Tb, yet emissions lines attributable to Pr are typically apparently absent. It is possible that the Sm^{3+} peaks at 593 and 639 plus the Eu^{3+} peak at 612 nm may be enhanced by the Pr^{3+} triplet located at 592, 615 and 637 nm. However, the relative intensities of the Eu and Sm peaks are expected to be far greater than those of Pr owing to their relatively greater efficiency of luminescence. The presence of Pr peaks could perhaps be revealed by spectrum-stripping methods. However, we consider that the application of such methods to CL spectra of apatite is premature, given that the nature of its CL activation remains incompletely understood (see below), and Pr lines in particular are subject to significant crystal-field effects.

Mariano (1978, 1988, 1989) has provided detailed interpretations of the spectra of blue and yellow apatite from carbonatites and granitic rocks, respectively. Here, we present spectra for apatite from the Coldwell alkaline

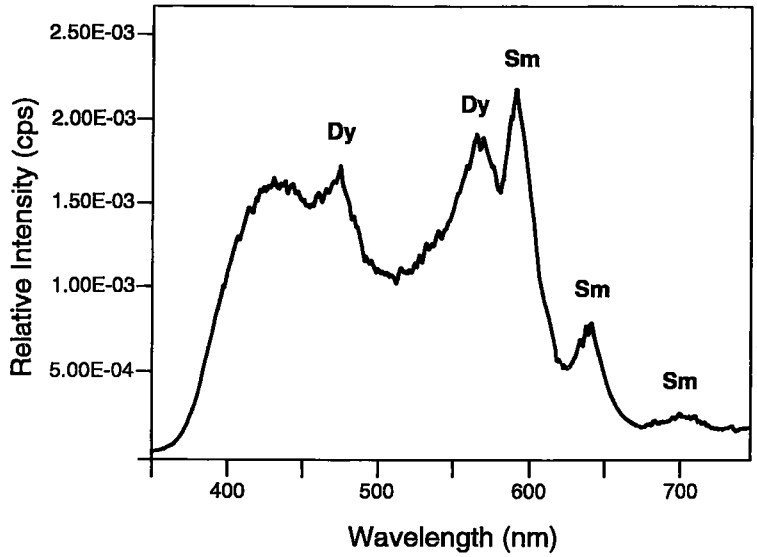

FIG. 11. CL spectrum of pink-violet-luminescent apatite in ferro-augite syenite from Center I of the Coldwell alkaline complex. Excitation conditions: 10 kV, 0.8 mA, 5-mm slits.

complex and from an Australian lamproite, which differ in some respects from previously published spectra of apatite.

Apatite from the Coldwell alkaline complex

The Coldwell alkaline complex contains both A-type oversaturated alkaline and peralkaline syenites and undersaturated nepheline syenites (Mitchell & Platt 1994). In most cases, the apatite in the oversaturated rocks from ferro-augite syenites of Center 1 is strongly zoned and exhibits a distinctive pink-to-violet luminescence (Xiong 1995). Most of these syenites exhibit relatively flat patterns of whole-rock *REE* distribution, with a significant negative Eu anomaly (Mitchell & Platt 1994). Patterns of *REE* distribution for apatite or other *REE*-bearing minerals in these rocks have not yet been determined.

Figure 11 illustrates a typical spectrum of pink-violet-luminescent apatite from ferro-augite syenite containing about 2 wt.% total $(REE)_2O_3$. The CL color arises from the presence of a broad band at 375–550 nm, coupled with poorly resolved complex peaks centered at about 590, 640 and 640 nm. These data may be interpreted as follows: the blue portion of the spectrum consists of a broad band due to Eu^{2+} and Ce activation, with a superimposed Dy peak. Intrinsic activation may also contribute to this portion of the spectrum. The region from 550 to 575 nm may reflect Mn activation; however, this region forms a continuum with the longer-wavelength portions of the blue band and the shorter wavelengths of the adjacent higher-energy *REE*-dominated band at 590 nm. Conventionally, the peaks at about 570 and 594 nm contributing to the continuum are interpreted to represent Dy and Sm activation, but the shape of the peaks, particularly the low-energy shoulder of the Sm peak, indicates clearly that other components may be present. Possible peaks include those of Eu^{3+} and Pr, although the latter is considered unlikely, given its low efficiency of luminescence relative to Eu. However, note that in this spectrum, it is impossible to identify conclusively any peaks due to Eu^{3+}; these are undoubtedly present, but are not resolved. Although Ce is the dominant *REE* (*ca.* 1 wt.% Ce_2O_3) in this sample of apatite, activation by Ce is not evident.

Figure 12 illustrates a spectrum of yellow-luminescent relatively *REE*-poor apatite [<1 wt. % total $(REE)_2O_3$], also from ferro-augite syenite. This spectrum is dominated by a Dy peak at about 475 nm and a complex peak at 575 nm, with a shoulder at 590 nm. In contrast to Figure 11, Eu^{2+} or Ce do not appear to be significant activators, even though Ce is again the dominant *REE* present. The peaks at 475 and 575 nm have relative intensities similar to those found in Dy-doped apatite (Fig. 5), indicating that Dy activation is mainly responsible for the overall CL color, and that Mn activation is not significant. The poorly resolved peak at 590 nm and the small peak at 640 nm are due to Sm activation. As in Figure 11, Eu^{3+} peaks cannot be identified. The small peak at 540 nm represents Tb activation. In contrast to the spectrum of the pink-luminescing apatite, this spectrum is dominated by heavy *REE* activators.

Figure 13 illustrates a spectrum of a yellow-red-luminescent (bronze) apatite [<2 wt.% $(REE)_2O_3$)], also from ferro-augite syenite. This spectrum is dominated by peaks of Dy and Sm, and Eu^{2+} or Ce are not significant

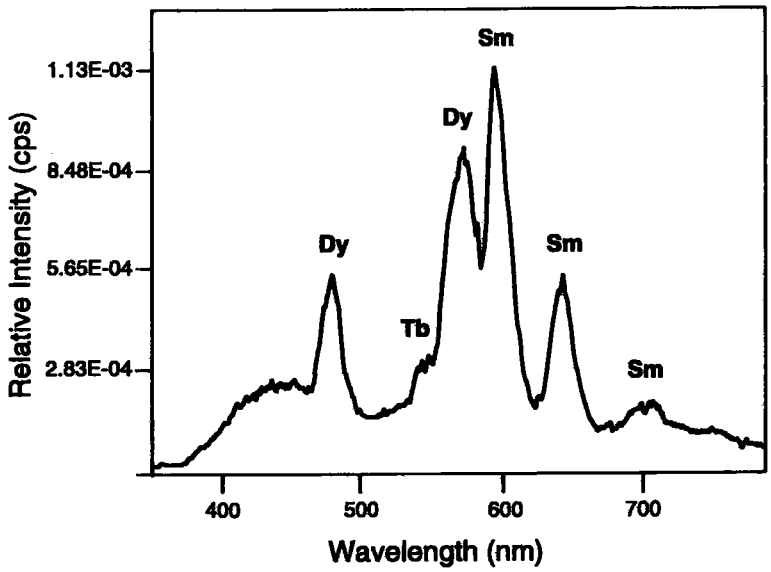

FIG. 12. CL spectrum of yellow-luminescent apatite in ferro-augite syenite from Center I of the Coldwell alkaline complex, Ontario. Excitation conditions: 10 kV, 0.8 mA, 5-mm slits.

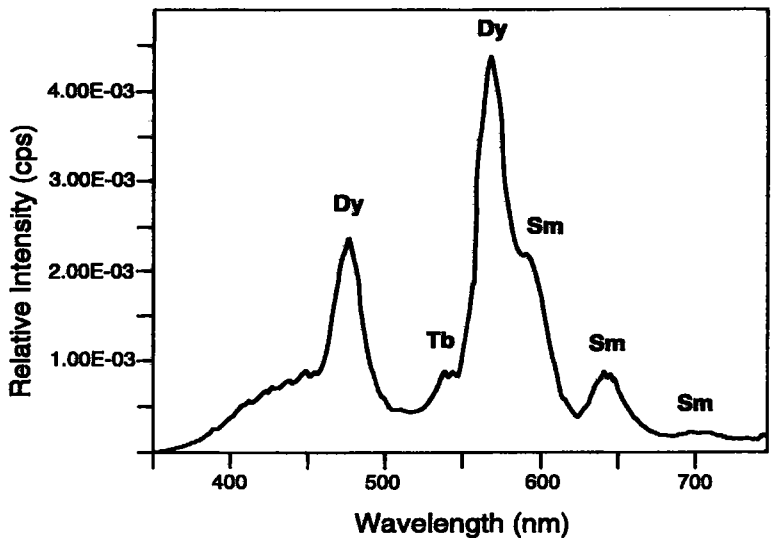

FIG. 13. CL spectrum of yellow-red-luminescent (bronze) apatite in ferro-augite syenite from Center I of the Coldwell alkaline complex, Ontario. Excitation conditions: 10 kV, 0.8 mA, 5-mm slits.

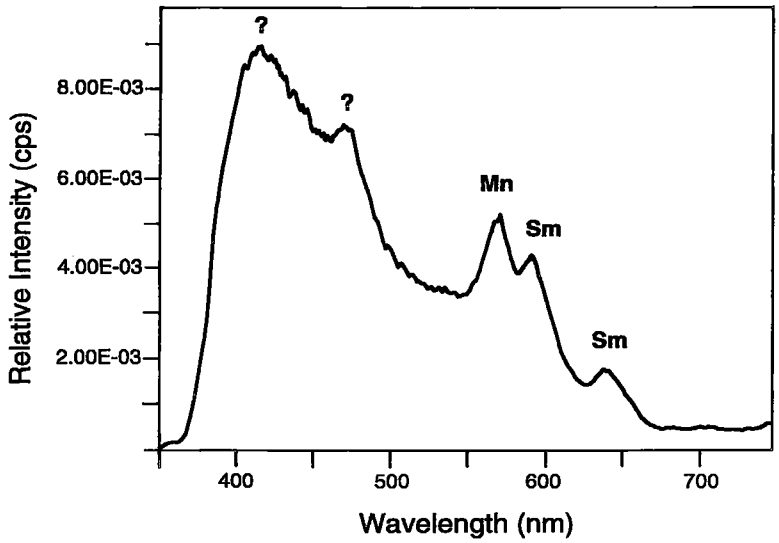

FIG. 14. CL spectrum of blue-luminescent Sr-rich, *REE*-poor apatite in from lamproite, Waldigee Hills, Australia. Excitation conditions: 10 kV, 0.8 mA, 5-mm slits.

activators, even though Ce is the dominant *REE* present. In contrast to the yellow apatite described above, the 575 nm Dy peak is clearly composed of several peaks, and the Sm peaks are of much greater intensity. Hence, the 558 nm Sm line appears as a prominent high-energy shoulder on the 575 nm Dy peak. The presence of a small Tb peak at 545 nm suggests that Mn activation appears to absent. The band at 694 nm suggests the presence of unresolved Eu^{3+} peaks at lower wavelengths.

These data show that apatite from the Coldwell ferroaugite syenite exhibits significantly different types of CL. These differences reflect changing *REE* distributions, which result from differentiation of the parental magma and from secondary metasomatic effects. Typically, yellow apatite occurs as a rim upon pink-violet apatite and records heavy *REE* enrichment in the late stages of magma evolution. Bronze apatite occurs in rocks that have undergone strong metasomatism involving the light *REE*.

Apatite in lamproite

Apatite in a pegmatitic lamproite from the Waldigee Hills, in Australia, exhibits light-violet luminescence. Crystals have a light-purple luminescent core and a purple yellow to dull purple luminescent rim that shows oscillatory zoning. The apatite contains 2–4 wt.% SrO and is poor in *REE* (not detectable by energy-dispersion analysis). The spectrum (Fig. 14) consists of an intense broad band (370–650 nm) with a maximum intensity at about 420 nm. Superimposed on this band are weak broad peaks at 570, 590, 640 nm, which may represent Dy and Sm activation. The peak at 470 nm cannot be assigned, and the 480 nm peak of Dy is undoubtedly hidden by the strong background continuum.

Similar violet-to-blue-luminescing zoned apatite in carbonatite has been described by Hayward & Jones (1991), who reported a correlation of Sr content with CL color. Unfortunately, they did not collect CL spectra. Despite the Sr–CL correlation, the intense band at 420 nm is unlikely to represent Sr activation, as all of the alkaline earth ions have never been demonstrated to be activators in any host. The CL spectra of other Sr-rich apatite (Roeder *et al.* 1987) do not contain this band. As the band cannot be correlated with any *REE* activator, it is possible that this unusual CL spectrum may reflect intrinsic luminescence due to deviations from stoichiometry or to the presence of structural defects.

CONCLUSIONS

The results of our study confirm that particular peaks in the CL spectra of apatite may be correlated with activation by a particular rare-earth element. However, the study of the relative efficiency of luminescence of the *REE* indicates that interpretation of the CL spectra of natural apatite may not be as straightforward as previously thought. Thus, the CL spectra of apatite doped with a single *REE* may not be entirely relevant to natural apatite, in which all of the *REE* occur together in diverse concentrations and proportions. In such an environment, crystal-field effects, co-enhancement, co-quenching and self-quenching undoubtedly occur, and it is these processes that determine the overall character and subtleties of the CL spectrum.

Thus, whereas it is possible to explain in a general

manner the origin of the yellow, blue and pink-violet CL of apatite derived from granite, carbonatite and peralkaline syenite, respectively, it is not possible to predict the observed spectra from the *REE* content of the apatite and the spectra of apatite doped with individual *REE*. Subtle variations in the ratio of quenching elements to strong emitters may significantly change the character of the CL spectrum, and it is these effects that account for the wide variation in the observed spectra of apatite derived from a particular paragenesis.

In summary, we believe that further advances in understanding the nature of CL in apatite will only be made by investigating synthetic apatite doped with diverse combinations of *REE*. For example, it would be important to establish the relative contributions of Sm and Pr to the 590 nm peak by study of apatite doped with these elements in various proportions. The roles of La, Ce, and Nd, which are commonly the dominant *REE* in apatite as CL co-enhancers or suppressors of the less abundant *REE*, need to be established. All of these data should be obtained on large single crystals of apatite in order that polarization effects and site distributions of the *REE* site may also be determined.

With regard to natural apatite, all further CL studies should include determination of the contents of all the *REE* and other potential activators (Mn, U) or suppressors (Fe) present in the sample investigated. Previous studies have not usually included these data, especially for the heavy *REE* and Eu, as they are not readily determined by electron-microprobe methods. Fortunately, technological advances in inductively coupled plasma methods of analysis now permit the determination of all 14 *REE* at low levels of concentration with relative ease. Thus, the relative concentrations of *REE*, and especially those of the very efficient activators such as Tb, Gd and Dy, may be usefully correlated with observed CL spectra.

Acknowledgements

This work was supported by the Natural Sciences and Engineering Research Council of Canada and Lakehead University. The technical assistance of Yuanming Pan, Ann Hammond and Sam Spivak is greatly appreciated. Reviews of this paper by Jorg Keller and John Hughes are greatly appreciated.

References

Axe, J.D. & Dieke, G.H. (1962): Calculation of crystal-field splitting of Sm^{3+} and Dy^{3+} levels in $LaCl_3$ with inclusion of J mixing. *J. Chem. Phys.* **37**, 2364-2371.

Blanc, P., Baumer, A., Cesbron, F. & Ohnenstetter, D. (1995): Les activateurs de cathodoluminescence dans les chlorapatites préparées par synthèse hydrothermale. *C.R. Acad. Sci. Paris, Sér.* **IIa, 321**, 119-126.

Blasse, A.C. & Bril, A. (1967): Investigation of Ce^{3+}-activated phosphors. *J. Chem. Phys.* **47**, 5139-5145.

Brecher, C., Samuelson, H. & Lempicki, A. (1967): The energy level structure of Eu^{3+} in YVO_4. *In* Optical Properties of Ions in Crystals (H.M. Crosswhite & H.W. Moos, eds.). Wiley Interscience, New York, N.Y. (73-83).

Buchanan, R.A., Wickersheim, K.A., Weaver, J.L., Sobon, L.E. & Anderson, E.E. (1967): Cathodoluminescence of rare earth-activated yttrium oxide. *In* 6th Rare Earth Res. Conf., Gatlinberg, Tennessee.

Crosswhite, H.M. & Dieke, G.H. (1961): Spectrum and magnetic properties of hexagonal $DyCl_3$. *J. Chem. Phys.* **35**, 1535-1548.

_____ & Moos, H.W. (1967): Crystal spectroscopy at the John Hopkins University. *In* Optical Properties of Ions in Crystals (H.H. Crosswhite & H.W. Moos, eds.). Wiley Interscience, New York, N.Y. (3-33).

DeShazer, L.D. & Dieke, G.H. (1963): Spectra and energy levels of Eu^{3+} in $LaCl_3$. *J. Chem. Phys.* **38**, 2190-2199.

Dieke, G.H. & Crosswhite, H.M. (1963): The spectra of the doubly and triply ionized rare earths. *Appl. Optics* **2**, 675-686.

Dornauf, H. & Heber, J. (1979): Fluorescence of Pr^{3+} ions in $La_{1-x}Pr_xP_5O_{14}$. *J. Luminescence* **20**, 271-281.

Drake, M.J. & Weill, D.F. (1972): New rare earth element standards for electron microprobe analysis. *Chem. Geol.* **10**, 179-181.

Dudkin, O.B., Krutikov, V.F., Faizullin, R.M. & Shcherbakov, V.D. (1994): EPR and photoluminescence spectra of apatite from the Khibiny deposits. *Zap. Vses. Mineral. Obshchest.* **123**, 94-104 (in Russ.).

Farok, H.M., Saunders, G.A., Lambson, W.A., Kruger, R., Senin, H.B., Bartlett, S. & Takel, S. (1996): An alexandrite effect and optical properties of holmium metaphosphate glass. *Phys. Chem. Glasses* **37**, 125-128.

_____, _____, Poon, W. & Vass, H. (1992): Low temperature fluorescence, valence state and elastic anomalies of samarium phosphate glasses. *J. Non-Crystalline Solids* **142**, 175-180.

Fleet, M. & Pan, Yuanming (1994): Site preference of Nd in fluorapatite [$Ca_{10}(PO_4)_6F_2$]. *J. Solid State Chem.* **112**, 78-81.

_____ & _____ (1995): Site preference of rare earth elements in fluorapatite. *Am. Mineral.* **80**, 329-335.

Freed, S. (1931): Electronic transitions between an inner shell and the virtual outer shells of the ions of the rare earths in crystals. *Phys. Rev.* **38**, 2122- 2130.

Gravely, B.T. (1970): Absorption, fluorescence and thermoluminescence in gamma- irradiated Pr^{3+}: LaF_3. *J. Chem. Phys.* **52**, 3610-3613.

Hayakawa, T., Kamata, N. & Yamada, K. (1996): Visible emission characteristics in Tb^{3+}-doped fluorescent glasses under selective excitation. *J. Luminescence* **68**, 179- 186.

HAYWARD, C.L. & JONES, A.P. (1991): Cathodoluminescence petrography of Middle Proterozoic extrusive carbonatite from Qasiarsuk, South Greenland. *Mineral. Mag.* **55**, 591-603.

HENDERSON, S.T. & RANBY, P.W. (1957): Cerium-activated halophosphate phosphors. *J. Electrochem. Soc.* **104**, 612-615.

HUAXIN, D. (1980): Cathodoluminescence of apatite. *Geochimica* **12**, 369-374 (in Chinese).

HUGHES, J.M., CAMERON, M. & MARIANO, A.N. (1991): Rare-earth-element ordering and structural variations in natural rare-earth-bearing apatites. *Am. Mineral.* **76**, 1165-1173.

ITO, J. (1968): Silicate apatites and oxyapatites. *Am. Mineral.* **53**, 890-907.

KELLER, S.P. (1958): Fluorescence spectra, term assignments and crystal field splitting of rare earth activated phosphors. *J. Chem. Phys.* **29**, 180-187.

LAGERWAY, A.A.F. (1977): Detection of trace elements in apatite crystals from Panasqueira, Portugal by non-destructive methods, especially polarspectrography. *Scripta Geologica (Leiden)* **42**.

LANG, R.J. (1936): The spectrum of trebly ionized cerium. *Can. J. Res.* **14**, 127- 130.

LAUD, K.R., GIBBONS, E.F., TIEN, T.Y. & STADLER, H.L. (1971): Cathodoluminescence of Ce^{3+}- and Eu^{3+}-activated alkaline earth feldspars. *J. Electrochem. Soc., Solid State Sci.* **118**, 918-923.

LECKEBUSCH, R. (1979): Comments on the luminescence of apatites from Panasqueria (Portugal). *Neues Jahrbuch Mineral., Monatsh.*, 17-21.

MAGNO, M.S. & DIEKE, G.H. (1962): Absorption and fluorescence spectra of hexagonal $SmCl_3$ and their Zeeman effects. *J. Chem. Phys.* **37**, 2354-2363.

MARFUNIN, A.S. (1979): *Spectroscopy, Luminescence and Radiation Centers in Minerals*. Springer Verlag, Berlin, Germany.

MARIANO, A.N. (1978): The application of cathodoluminescence for carbonatite exploration and characterization. *In* Proc. First Int. Symp. on Carbonatites (C.J. Braga, ed.). Brazil Departamento Nacional da Producão Mineral, Brasilia, Brazil (39-57).

_____ (1988): Some further geological applications of cathodoluminescence. *In* Cathodoluminescence of Geological Materials (D.J. Marshall, ed.). Unwin Hyman, Boston, Massachusetts (94-123).

_____ (1989): Cathodoluminescence emission spectra of rare earth element activators in minerals. *In* Geochemistry and Mineralogy of Rare Earth Elements (B.R. Lipin & G.A. McKay, eds.). *Rev. Mineral.* **21**, 339-348.

_____ & RING, P.J. (1975): Europium-activated cathodoluminescence in minerals. *Geochim. Cosmochim. Acta* **39**, 649-660.

MITCHELL, R.H. & PLATT, R.G. (1994): Field guide to aspects of the petrology of the Coldwell alkaline complex. *Geol. Assoc. Can. – Mineral. Assoc. Can., ???.*

MOROZOV, A.M., MOROZOVA, L.G., TREFIMOV, A.K & FEOFILOV, P.P. (1970): Spectral and luminescent characteristics of fluoroapatite single crystals activated by rare earth ions. *Optics and Spectroscopy* **29**, 590-596.

NAZAROVA, V.P. (1961): Cathodoluminescence of europium activated strontium phosphates. *Akad. Nauk SSSR, Bull. Phys. Ser.* **25**, 322-324.

OVCHARENKO, V.K. & YU'EV, L.D. (1971): Luminescence of Ukrainian apatites. *Dopov. Akad. Nauk Ukrainian SSR, Ser.* **B**, **33**, 974-977 (in Ukrainian).

OZAWA, J. (1990): *Cathodoluminescence: Theory and Applications.* Kodansha, Tokyo, Japan.

PALILLA, F.C. & O'REILLY, B.E. (1968): Alkaline earth halophosphate phosphors activated by divalent europium. *J. Electrochem. Soc.* **115**, 1076-1081.

PELLETIER-ALLARD, N., PELLETIER, R. & TISEANUE, C. (1994): Quenching process of the Nd fluorescence in Nd, Er codoped yttrium aluminium perovskite. *J. Luminescence* **62**, 257-262.

PORTNOV, A.M. & GOROBETS, B.S. (1969): Luminescence of apatite from different rock types. *Dokl. Akad. Nauk SSSR* **184**, 110-113.

RAST, H.E., FRY, J.L. & CASPERS, H.H. (1967): Energy levels of Sm^{3+} in LaF_3. *J. Chem. Phys.* **46**, 1460-1466.

ROEDER, P.L. (1985): Electron microprobe analysis of minerals for rare earth elements: use of calculated peak-overlap corrections. *Can. Mineral.* **23**, 263-271.

_____, MACARTHUR, D., MA, XIN-PEI, PALMER, G.R. & MARIANO, A.N. (1987): Cathodoluminescence and microprobe study of rare-earth elements in apatite. *Am. Mineral.* **72**, 801-811.

ROPP, R.C. (1964): Spectral properties of rare earth oxide phosphors. *J. Electrochem. Soc.* **111**, 311-317.

SAYRE, E.V. & FREED, S. (1955): Absorption spectrum and quantum states of the praseodymium ion. II. Anhydrous praseodymium fluoride in films. *J. Chem. Phys.* **23**, 2066-2068

_____, SANCIER, K.M. & FREED, S. (1955): Absorption spectrum and quantum states of the praseodymium ion. I. Single crystals of praseodymium chloride. *J. Chem. Phys.* **23**, 2060-2065.

STEINBRUEGGE, K.B., HENNIGSEN, T., HOPKINS, R.H., MAZELSKY, R., MELAMED, N.T., RIEDEL, E.P. & ROLAND, G.W. (1972): Laser properties of Nd^{3+} and Ho^{3+} doped crystals with the apatite structure. *Appl. Optics* **11**, 999-1012.

TANABE, S., SUZUKI, K., SOGA, N. & HANADA, T. (1995): Mechanics and concentration dependence of Tm^{3+} blue and Er^{3+} green up-conversion in codoped glasses by red-laser pumping. *J. Luminescence* **65**, 247-255.

TODA, K., HONMA, T. & SATO, M. (1997): Unusual concentration quenching of europium luminescence in a new layered perovskite compound $RbLa_{1-x}Eu_xTa_2O_7$. *J. Luminescence* **71**, 71-75.

VAN UITERT, L.G. & JOHNSON, L.F. (1966): Energy transfer between rare earth ions. *J. Chem. Phys.* **44**, 3514-3522.

WEBER, M.J. & BIERIG, R.W. (1964): Paramagnetic resonance and relaxation of trivalent rare-earth ions in calcium fluoride. I. Resonance spectra and crystal fields. *Phys. Rev.* **134A**, 1492-1503.

WYBOURNE, B.G. (1962): Structure of f^n configurations. II. f^5 and f^9 configurations. *J. Chem. Phys.* **36**, 2301-2311.

XIONG, JIAN (1995): *Cathodoluminescence Studies of Feldspars and Apatites from the Coldwell Alkaline Complex.* M.Sc. thesis, Lakehead Univ., Thunder Bay, Ontario.

Received August 15, 1996, revised manuscript accepted May 10, 1997.